J Sol-Gel Sci Technol (2015) 73:127–132
DOI 10.1007/s10971-014-3503-5

ORIGINAL PAPER

Corrosion resistance of sol–gel alumina coated Mg metal in 3.5 % NaCl solution

I. B. Singh · Prasant Gupta · Arpit Maheshwari · Naveen Agrawal

Received: 1 August 2014 / Accepted: 7 September 2014 / Published online: 16 September 2014

Abstract This investigation describes the potential of sol–gel derived alumina coating on the corrosion resistance of magnesium metal in 3.5 % NaCl solution. Coating deposition was performed by dip coating technique using boehmite (AlOOH) sol followed by their sintering at 250 °C. EDX and FTIR analysis confirmed that alumina is a main constituent of the coating. Microstructural examination of the coated surface demonstrated amorphous nature of coating of 2–3 μm in thickness. Potentiodynamic polarization and electrochemical impedance measurements indicated a considerable improvement in the corrosion resistance of the coated substrates.

Keywords Mg metal · Alumina coating · EDX · FE-SEM · EIS · FTIR

1 Introduction

Magnesium-based alloys posses an attractive combination of low density, high strength/weight ratio and good castability. Due to these properties, they are being considered as a suitable substitute of ferrous alloys/aluminium in automotive and aerospace applications [1–3]. Unfortunately, they are highly susceptible to corrosion, particularly in humid air and chloride bearing wet environment. Presence of lowest electrode potential than other metals is another problem with the Mg alloys for the occurrence of galvanic corrosion. These problems have limited their use in various applications. To control their corrosion, development of an effective corrosion resistance coating can be a viable solution. Earlier several types of coating techniques like anodizing, electrochemical plating, chemical conversion, hybrid organic coating etc. have been applied on Mg and their alloys [4–15]. However, each method is having their own advantages and disadvantages. For e.g., uneven distribution of current density in the plating bath results in non uniform plating of complex shaped structure in electrochemical plating [6].

Among various developed coatings, rather recently developed sol–gel process based ceramics coatings are found to be more effective. Sol–gel route of coating development is mainly consists of the formation of ceramic oxide films through successive reactions of hydrolysis and condensation of the precursors [16, 17]. Coatings developed through this technique offer many advantages, i.e. better adhesion, low surface preparation and processing temperatures, use of relatively simple and inexpensive equipment. In addition, coating can be applied easily using deep coating technique of any complex shaped substrate. Initially, researchers were concerned in the development of sol–gel process based coatings on steels substrate. This resulted the development of coatings of ceramics oxides such as SiO_2, ZrO_2, SiO_2/TiO_2, ZrO_2/Y_2O_3, ZrO_2/CeO_2, Al_2O_3 etc. on the different types of steel and stainless steel substrates [18–27]. Singh et al. [28–30] observed a significant improvement in the corrosion and pitting resistances of sol–gel alumina coated low carbon steel, 9Cr 1Mo ferritic steel and 304 SS in highly corrosive NaCl solution. In comparison, relatively few study has been reported in the development of sol–gel based ceramic oxides coating on Mg alloys [31–36]. Phani et al. [35] developed sol–gel ZrO_2 and ZrO_2–CeO_2 coatings on Mg based AZ91D and AZ31alloys. They found that both coated alloys showed superior corrosion performance in

I. B. Singh (✉) · P. Gupta · A. Maheshwari · N. Agrawal
Material Characterization Group, CSIR-Advanced Materials and Process Research Institute, Bhopal 462064, M.P., India
e-mail: ibsingh58@yahoo.com

salt spray test. In the recent investigation, sol–gel based composite organic coatings deposited on Mg–Zn–Ca alloy used in clinical application [36]. As per our knowledge, none of investigation reports the development of sol–gel coatings particularly alumina coating on Mg metal.

In views of above statement, present investigation was aimed to employ development of sol–gel alumina coating on Mg metal and evaluate their corrosion 3.5 % NaCl solution. Observed results indicates that sol–gel-derived Al_2O_3 coating on Mg metal reduces their corrosion rate an order of magnitude lower than uncoated Mg in 3.5 % NaCl solution.

2 Experimental

2.1 Specimen preparation

Specimens used for coating developments, were cut from Mg sheet (~ 99 % purity) of 3 mm × 10 mm × 10 mm of dimension. After polishing with different grades of emery paper, specimens were degreased properly with trichloroethylene solution.

2.2 Synthesis of boehmite sol and coating deposition

Boehmite (AlOOH) sol was prepared by mixing Al-isopropoxide and water in their 1:100 molar ratio. The suspension was refluxed and stirred vigorously at 85 °C for 4–5 h until it converted into a clear sol. Details of synthesis of boehmite sol is available elsewhere [27–29]. Viscosity of the sol was measured as 1.58 mPa s using a Brookfield R/S plus rheostat at shear rate of 600 s^{-1}. The synthesized boehmite sol was then utilized for coating development. Coating was applied at prepared specimens using dip coating technique of a constant withdrawal speed of 1 cm/s (approx). Finally, air dried coated specimens were heated at 250 °C in oven for 3 h.

2.3 Microstructural and compositional analysis

Microstructural and compositional analysis of the coatings was made with the help of Field Emission Scanning Electron Microscope (FE-SEM) (NOVA Nano SEM 430) equipped with EDS. The Presence of functional groups in the coatings was analyzed using FTIR (Model Nicolet 5700) in a frequency range of 700–4,000 cm^{-1}.

2.4 Electrochemical measurements

Open circuit potential (OCP), potentiodynamic polarization and electrochemical impedance spectroscopy (EIS) were carried out using a conventional three electrodes (a saturated calomel electrode (SCE) as reference electrode, platinum plate as counter electrode and test specimens as working electrode) system bearing electrochemical cell. All the electrochemical measurements were made in 3.5 % NaCl solution at room temperature (30 ± 2 °C) using computer controlled Solatron 1280 Z corrosion system equipped with Corrware and Zplot softwares. Tafel plots were obtained by carrying out potentiodynamic polarization at a constant scan rate of 1 mV/s at ± 150 mV from OCP. Impedance analysis were made in a frequency range of 20 kHz to 0.01 Hz at OCP by applying a sine potential signal of 10 mV. Different parameters related to potentiodynamic polarization and impedance measurements were derived by curve fitting method using Corrview and Zview software, respectively. Each experiment has been repeated two to three times to confirm reproducibility of the results.

3 Results and discussion

3.1 Elemental and microstructure analysis

Figure 1 reveals the surface topography through the coated and uncoated parts from the same specimen. The coated part can be distinguished with the presence of a thick layer as compared to uncoated part of the specimen. Elemental X-ray mapping of aluminum (Al) and oxygen (O) through the coating as depicted in Fig. 1, exhibits their a considerable presence. However, their concentration becomes very low at the uncoated part of the specimen. In case of magnesium (Mg), elemental mapping demonstrates their presence in the bulk level at the uncoated part. But their concentration becomes very less the coated part (Fig. 1). EDS analysis of Al, O, Mg elements was made to quantify their presence in the coated and uncoated parts of the substrate. EDS analysis as presented in Table 1, show a higher concentration of Al (27 wt%) and O (52 wt%) and very low concentration of Mg (<2 wt%) at the coated part. This analysis evidenced the presence of alumina in the coating.

Figure 2 shows a magnified view of the coated surface though the plane and the cross section. The morphology of the coating as depicted in Fig. 2b, shows jelly like appearance of the coating. In the cross sectional view (Fig. 2c), coating can be differentiated as a white layer of 2–3 μm in thickness. Coating appears amorphous in nature which is free from the cracks and porosities.

3.2 FTIR analysis

Figure 3 illustrates the FTIR spectra of boehmite (aluminium oxy-hydroxide) coated surface of the substrate. Presence of a broad band in the spectral range 3,200–3,500 cm^{-1} is mainly due to –OH stretching of hydrogen

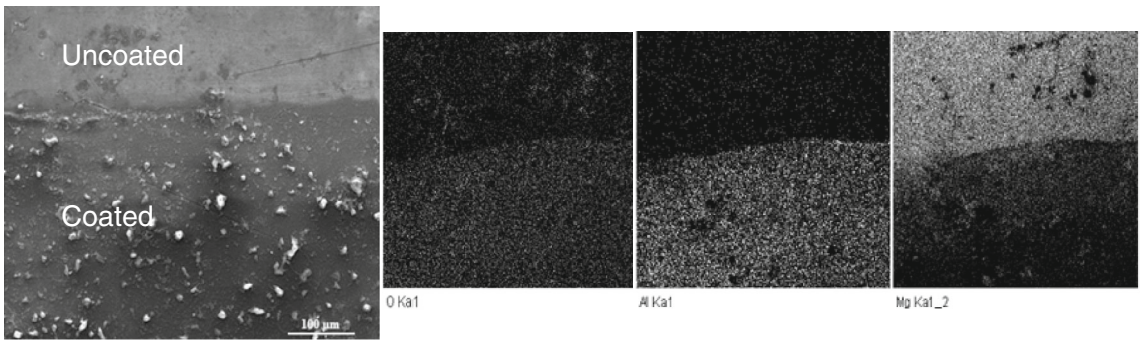

Fig. 1 Elemental X-ray mapping of Al, O, Mg through the alumina coated and uncoated Mg surfaces

Table 1 EDX analysis of Mg metal and double layered alumina coated Mg surface

Elements	Mg metal (wt%)	Coated Mg surface (wt%)
C	10.79	14.49
O	6.67	52.95
Mg	82.88	1.71
Al	0.56	27.86
Si	0.28	1.62

bonded aluminium oxy-hydroxide (AlO(OH) [37, 38]. Since complete oxidation of boehmite into γ alumina occurs at 450 °C and above temperatures [38], presence of trace of unoxidized boehmite can not be ruled out. Occurrence of a small broad band at 2,100–2,000 cm^{-1} spectral range is mainly related to the presence of hydrogen bonded OH group [38]. This evidences the presence of water molecules in the coating. The occurrence of next small absorption peak at further low intensity at 1,384 cm^{-1} is due to stretching of Al–C bond that correspond to alkyl (ethoxy) group of the precursor. Presence of organic groups is reported to help in reducing the stresses and cracks in the coating [39, 40]. Origin of small peak at 1,070 cm^{-1} is also correspond to boehmite [38]. A steep increase of absorption at 800 cm^{-1} is belongs to Al–O vibration mode of Al_2O_3 [37, 38, 41]. Absorption related to Al–O vibration is mainly due to presence of alumina in their different phases [42, 43]. Present FTIR measurement indicates that the most of the boehmite present in the coating get oxidized into alumina after heating at 250 °C as per following reaction (1).

$$2\,Al(OOH) \rightarrow Al_2O_3 + H_2O \quad (1)$$

Due to heating at lower temperature, trace of the unoxidized boehmite, residual precursor along with molecular water were also analyzed in the coating. However, their presence did not make any adverse effect toward the stability/adherence of the coating.

3.3 Electrochemical corrosion evaluation

3.3.1 Open circuit potential (OCP)

The steady state of OCPs measured after 30 min of exposure in 3.5 % NaCl solution, are given in Table 2. From the trend, it can be noticed that OCP of the coated specimen occurs more positive than that of the uncoated specimen. OCP of the single layered coated specimen was found more than 30 mV positive than the uncoated specimen while OCP of the double layered coated specimen increased 75 mV positive −1.515 V than OCP measured for the

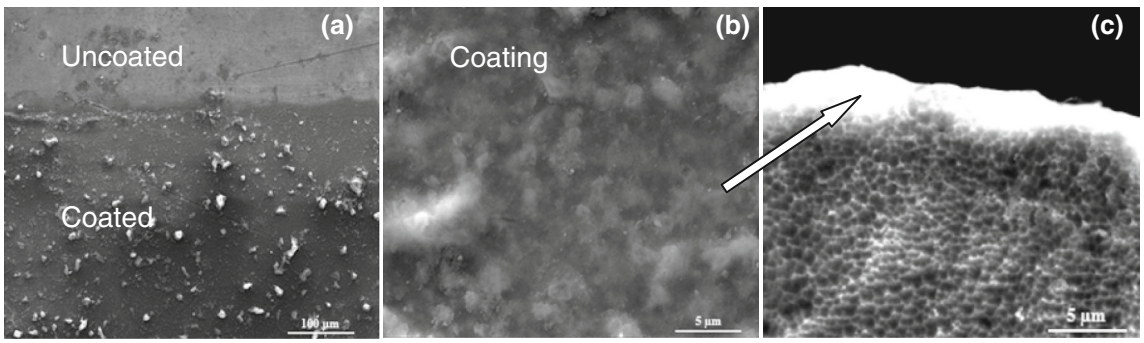

Fig. 2 Microstructure of alumina coating through **a** coated and uncoated surface, **b** coated surface at higher magnification, **c** cross section of coated specimen

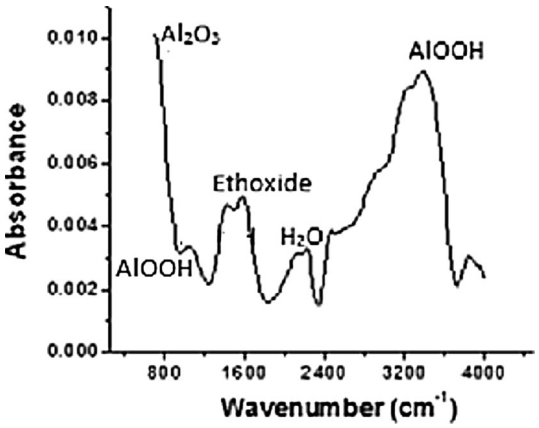

Fig. 3 FTIR spectra of boehmite coated Mg after heating at 250 °C

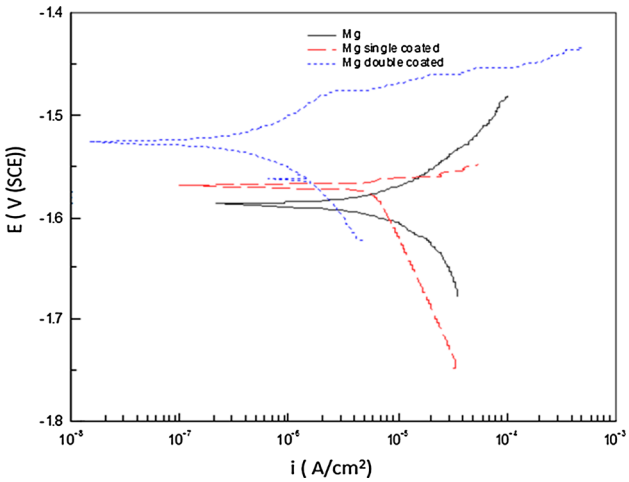

Fig. 4 Tafel plots for Mg alone and single and double layered alumina coated Mg surface in 3.5 % NaCl solution

uncoated specimen (−1.59 V). OCP measurement suggests the presence of the alumina coating over Mg surfaces shift their equilibrium potential in noble direction.

3.3.2 *Tafel plots*

Tafel plots were obtained by carrying partial potentiodynamic polarization in the potential range of ±150 mV from the OCP. Tafel plots as given in Fig. 4, were recorded for all the thee types of studied specimen (Mg alone, Mg single layered alumina coated and double layered alumina coated) in 3.5 % NaCl solution. Different parameters like corrosion current density (I_{corr}), cathodic (β_c) and anodic (β_a) Tafel constants obtained from the Tafel plots, are summarized in Table 2. I_{corr} was derived after extrapolation of anodic and cathodic polarization curves. I_{corr} is overall current flow as a result of onset of the anodic (oxidation) and cathodic (reduction) reactions. According to measured results as presented in Table 2, I_{corr} of Mg metal (uncoated) occurs more than two times higher than single layered coated specimen while I_{corr} of the double layered coated specimen becomes one order of magnitude lower than Mg metal. Measurement of comparatively a higher values of β_a and β_c of the coated specimens as compared to uncoated specimen suggests the developed alumina coating control both, anodic and cathodic reactions. Occurrence of an order of magnitude lower I_{corr} for double layered alumina coated specimen than uncoated specimen indicates that double layered coating impart better corrosion protection.

3.3.3 *Electrochemical impedance spectroscopy (EIS)*

Electrochemical impedance spectroscopy measurements were performed for all the three types of studied specimens at their OCP. The observed EIS spectra in their Nyquist plot form, are shown in Fig. 5. From the EIS diagrams, it can be seen that all the specimens show the occurrence of a depressed semi circles with presence of capacitive loop. The radius of the capacitive semicircle increase with the increase of coated layer. It occurs minimum for Mg metal while maximum for double layered coated surface. Another interesting point to be noted here that Mg metal and single layered alumina coated specimen show the existence of inductive loop (just above the real axis) in the lower frequency region. Though, the occurrence of inductive behavior is much more pronounced in Mg metal. In case of double layered alumina coated specimen, inductive

Table 2 Different electrochemical parameters derived by Tafel extrapolation

Electrom. parameters	Mg uncoated	Mg single coated	Mg double coated
OCP (mV, SCE)	−1,588 ± 10	−1,560 ± 10	−1.526 ± 10
I_{corr} (A/cm^2)	6.35 ± 0.2 × 10^{-6}	2.50 ± 0.2 × 10^{-6}	4.76 ± 0.2 x 10^{-7}
β_a (mV/decade)	58.2 ± 5	62.8 ± 5	68.3 ± 5
β_c (mV/decade)	−127 ± 5	−134 ± 5	−142 ± 5
R_{ct} (Ωcm^2)	2,175 ± 3 %	2,775 ± 5.3 %	4,250 ± 4.8 %
C_{dl} (F/cm^2)	2.1739 × 10^{-6}	1.162 × 10^{-6}	1.0584 × 10^{-6}
R_s (Ωcm^2)	72.01 ± 3.5 %	74.1 ± 3.35 %	86.8 ± 5.65 %

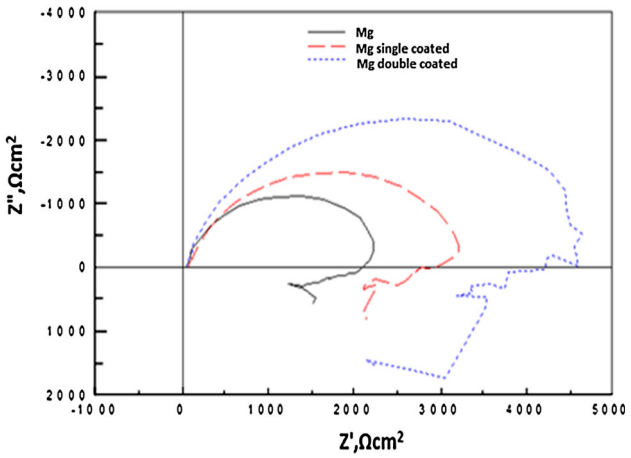

Fig. 5 EIS (Nyquist plots) Mg alone and single and double layered alumina coated Mg metal in 3.5 % NaCl solution

behavior is insignificant. The occurrence of such behavior in the Nyquist diagram is the consequence of adsorption of anions [44]. It may therefore be inferred that the adsorption of Cl^- ions occurs with very fast rate at the Mg metal as compared to alumina coated surfaces.

Different parameters like charge transfer resistance (R_{ct}), electrical double layer capacitance (C_{dl}) and solution resistance (R_s) derived by curve fitting method, are given in Table 2. Because of the occurrence of single semi circle in the Nyquist plots, an equivalent circuit consisting of resistor connected in series to a parallely connected resistor and capacitor has been used for data analysis. Measurement of more than two times higher R_{ct} values of double layered alumina coated Mg (4,250 Ωcm^2) than Mg metal alone (2,175 $\Omega cm^{2)}$ indicates the effectiveness of alumina in increasing of corrosion resistances of magnesium. A higher R_{ct} ultimately responsible for the reduction in diffusion process through the coating/metal interfaces. Single layered alumina coated Mg has also shown a significant increase ($\sim$25 %) in their R_{ct} values as compared to Mg metal. A fast rate of diffusion of oxidized Mg^{2+} ions at the metal oxide/solution interface is the reason for the occurrence of a lowest R_{ct} value for the Mg metal. Measurement of a higher value of C_{dl} for the Mg metal as compared to coated specimens is due to an increase of dielectric constant. Penetration of the electrolyte through cracks and pores increase the dielectric constant of the interfaces [45]. This suggest that presence of porous oxide layer at the Mg surfaces increases diffusion process. The measured solution resistance as given in Table 2, also in accordance with charge transfer resistance measurement. A comparatively higher value of R_s for double layered alumina coated specimen as compared to Mg alone indicate that former one posses a better resistant surfaces. Present EIS results are in good agreement with the corrosion rate measured by the Tafel plots.

4 Conclusions

1. Sol–gel based alumina coatings developed at the Mg surface reduces their corrosion rate an order of magnitude lower in 3.5 % NaCl solution.
2. EDX, X-ray mapping and FTIR analysis evidence the presence of Al_2O_3 layer at the coated Mg surface
3. Microstructural studies of the coated surface suggests the presence of cracks free amorphous alumina layer of around 2–3 μm in thickness.
4. EIS analysis indicates alumina coated layer acts as barrier layer between metal/solution interfaces that control the diffusion phenomena up to maximum level.

Acknowledgments Authors are thankful director, CSIR-AMPRI for providing laboratory facilities. They are also thankful to Mr. A. K. Khare for EDS analysis.

References

1. Cao FH, Len VH, Zhang Z, Zhang JQ (2007) Corrosion behavior of Mg and its alloy in NaCl solution. Russ J Electrochem 47:837–843
2. Baril G, Pebere N (2001) The corrosion of pure magnesium in aerated and de-aerated sodium sulphate solution. Corros Sci 43:471–484
3. Makar GL, Kruger AJ (1990) Corrosion studies of rapidly solidified magnesium alloys. J Electrochem Soc 37:414–421
4. Hwang DY, Kim YM, Shin DH (2009) Corrosion resistance of plasma-anodized AZ91 Mg alloy in the electrolyte with/without potassium fluoride. Mater Trans 50:671–678
5. Jamesh MI, Zhao Y, Wu G, Jin W, McKenzie DR, Bilek MM, Chu PK (2014) Effects of zirconium and nitrogen plasma immersion ion implantation on the electrochemical corrosion behavior of Mg–Y–RE alloy in simulated body fluid and cell culture medium. Corros Sci 86:239–261
6. Gray JE, Luan B (2002) Protective coatings on magnesium and its alloys. J Alloys Compd 336:88–113
7. Song GL, Shi Z (2014) Corrosion mechanism and evaluation of anodized magnesium alloys. Corros Sci 85:126140
8. Song S, Shen WD, Liu MH, Song GL (2012) Corrosion study of new surface treatment/coating for AZ31B magnesium alloy. Surf Eng 28:486–490
9. Fini MH, Amadesh A (2013) Improvement of wear and corrosion resistance of AZ91 magnesium alloy by applying Ni–SiC nanocomposite coating via pulse electrodeposition. Trans Nonferr Met Soc China 23:2914–2922
10. Shashikala AR, Umarani R, Mayanna SM, Sharma AK (2008) Chemical conversion coatings on magnesium alloys—a comparative study. Int J Electrochem Sci 3:993–1004
11. Kartsonakis IA, Balaskas AC, Koumoulos EP, Charitidis CA, Kordas G (2012) Evaluation of corrosion resistance of magnesium alloy ZK10 coated with hybrid organic–inorganic film including containers. Corros Sci 65:481–493

12. Jin F, Chu PK, Xu G, Zhao J, Tang D, Tong H (2006) Structure and mechanical properties of magnesium alloy treated by micro-arc discharge oxidation using direct current and high-frequency bipolar pulsing modes. Mater Sci Eng A 435–436:123–126
13. Hu W (2012) Protective diffusion coatings on magnesium alloys: a review of recent developments. J Alloys Compd 520:11–21
14. Senf A, Broszei E (1999) Wear and corrosion protection of aluminum and magnesium alloys using chromium and chromium nitride PVD coatings. Adv Eng Mater 1:133–137
15. Liu DM, Troczynski T, Tseng WJ (2001) Water-based sol–gel synthesis of hydroxyapatite: process development. Biomaterials 22:1721–1730
16. Zhang S, Li Q, Fan J, Kang W, Yang X (2009) Novel composite films prepared by sol–gel technology for the corrosion protection of AZ91D magnesium alloy. Prog Org Coat 66:328–335
17. Ćurković L, Ćurković HO, Salopek S, Renjo MM, Šegot S (2013) Enhancement of corrosion protection of AISI 304 stainless steel by nanostructured sol–gel TiO_2 films. Corros Sci 77:176–184
18. Tiwari SK, Tripathi M, Singh R (2012) Electrochemical behavior of zirconia based coatings on mild steel prepared by sol–gel method. Corros Sci 63:334–341
19. Salahinejad E, Hadianfard MJ, Macdonald DD, Mozafari M, Vashaee D, Tayebi L (2013) A new double-layer sol–gel coating to improve the corrosion resistance of a medical-grade stainless steel in a simulated body fluid. Mater Lett 97:162–165
20. Dias SAS, Lamaka SV, Nogueira CA, Diamantino TC, Ferreira MGS (2012) Sol–gel coatings modified with zeolite fillers for active corrosion protection of AA2024. Corros Sci 62:153–162
21. Ramírez-del-Solar M, Esquivias L, Craievich AF, Zarzycki J (1992) Ultrastructural evolution during gelation of TiO_2-SiO_2 sols. J Non Cryst Solids 147–148:206–212
22. Giampaolo Conde ARD, Puerta M, Ruiz H, Olivares JL (1992) Thick aluminosilicate coating on carbon steel via sol–gel. J Non Cryst Solids 147:468–474
23. Guglielmi M, Festa D, Innocenzi PC, Colombo P, Gobbi M (1992) Borosilicate coatings on mild steel. J Non Cryst Solids 147:474–477
24. Shane M, Macartney ML (1990) Sol–gel synthesis of zirconia barrier coatings. J Mater Sci Lett 25:1537–1544
25. Miyazawa K, Suzuki K, Wey MY (1996) Microstruclure and oxidation-resistant property of sol–gel-derived Zr02–Y201 films prepared on austenitic stainless steel substrates. J Am Ceram Soc 78:347–357
26. Maggio RD, Fedrizzi L, Russ R, Scardi P (1996) Dry and wet corrosion behaviour of AISI R.D. 304 stainless steel coated by sol–gel ZrO_2–CeO_2. Thin Solid Films 286:127–135
27. Wang D, Bierwagen GP (2009) Sol–gel coatings on metals for corrosion protection. Prog Org Coat 64:327–338
28. Ruhi G, Modi OP, Singh IB (2009) Pitting of AISI 304 SS coated with nano structured sol–gel alumina coating in chloride containing acidic environment. Corros Sci 51:3057–3063
29. Ruhi G, Modi OP, Singh IB (2009) Corrosion behaviour of nano structured sol-gel alumina coated 9Cr–1Mo ferritic steel in chloride bearing environment. Surf Coat Technol 204:359–365
30. Ruhi G, Modi OP, Singh IB (2009) Effect of sintering atmosphere on the corrosion and wear resistance of sol–gel alumina coated mild steel surface. Corrosion 65:758–764
31. Ardelean H, Marcus P, Fiaud C (2001) Enhanced corrosion resistance of magnesium and its alloys through the formation of cerium (and aluminium) oxide surface films. Mater Corros 52:887–889
32. Wilson S, Howthrone HM, Yang Q, Troczynsk T (2000) Sliding and abrasive wear of composite sol–gel alumina coated alloys. Surf Coat Technol 133(389):396
33. Gao JH, Shi XY, Yang B, Hou SS, Meng EC, Guan FX, Guan SK (2011) Fabrication and characterization of bioactive composite coating on Mg–Zn–Ca alloy by MAO/sol–gel. J Mater Sci Mater Med 22:16811687
34. Wang H, Akid R, Gobara M (2010) Scratch-resistant anticorrosion sol–gel coating for the protection of AZ31 magnesium alloy via a low temperature sol–gel route. Corros Sci 52:256–2570
35. Phani AR, Gammel FJ, Hack T, Haefke H (2005) Enhanced corrosion resistance by sol-gel based ZrO_2–CeO_2 on magnesium alloys. Mater Corros 56:77–82
36. Hernández-Barrios CA, Duarte NZ, Hernández LM, Pena DY, Coy AE, Viejo F (2013) 2nd international meeting for researchers in materials and plasma technology. J Phys Conf Ser 466:012011
37. Venkatesh R, Ramanan SR (2000) Effects of organic additive on the properties of sol–gel spun micro alumina fibers. J Eur Ceram Soc 20:2543–2548
38. Saraswathi V, Rao GVR (1987) Structural evolution in alumina gel. J Mater Sci 22:2529–2534
39. Gallardo G, Duran A, Danberenea JJ (2004) Electrochemical and vitro behaviour of sol–gel coated 316 stainless steel. Corros Sci 46:795–806
40. Ruhi G, Modi OP, Sinha ASK, Singh IB (2008) Effect of sintering temperatures on corrosion and wear properties of sol–gel alumina coatings on surface pre-treated mild steel. Corros Sci 50:639–649
41. Meher T, Basu AK, Ghatak G (2005) Physicochemical characteristics of alumina gel in hydroxyhydrogel and normal form. Cer Int 31:831–838
42. Colomban P (1989) Structure of oxide gel and glasses by IR and Raman scattering: aluminas. J Mater Sci 24:3002–3010
43. Low M, Pherson RM (1989) Crystallization of gel derived by alumina and alumina–zirconia ceramics. J Mater Sci 24:892
44. Keddam M, Kurtz C, Takenouti H, Scuster D, Zuili D (1997) Exofoliation of corrosion of Al alloy examined by electrode impedance. Electrochim Acta 42:87–97
45. Peber N, Picaud T, Duprat M, Dabosi F (1989) Evaluation of corrosion performance of coated steel by the impedance technique. Corros Sci 29:1073–1079